

# Variational algorithms for linear algebra

Xiaosi Xu,<sup>1</sup> Jinzhao Sun,<sup>2</sup> Suguru Endo,<sup>1</sup> Ying Li,<sup>3</sup> Simon C. Benjamin,<sup>1</sup> and Xiao Yuan<sup>1,\*</sup>

<sup>1</sup>*Department of Materials, University of Oxford, Parks Road, Oxford OX1 3PH, United Kingdom*

<sup>2</sup>*Clarendon Laboratory, University of Oxford, Parks Road, Oxford OX1 3PU, United Kingdom*

<sup>3</sup>*Graduate School of China Academy of Engineering Physics, Beijing 100193, China*

(Dated: December 21, 2024)

Quantum algorithms have been developed for efficiently solving linear algebra tasks. However they generally require deep circuits and therefore universal fault-tolerant quantum computers. In this work, we propose variational algorithms for linear algebra tasks that are compatible with Noisy Intermediate Scaled Quantum devices. We show that the solutions of linear systems of equations and matrix-vector multiplications can be translated as the ground states of the constructed Hamiltonians. Based on recently proposed variational quantum algorithms, we introduce Hamiltonian morphing together with an adaptive ansatz for efficiently finding the ground state. As the ground state always has zero energy, it also enables us to verify the solution. Our algorithms have wide applications in machine learning and optimisation problems, and the algorithm for matrix multiplications can be also used for variational Hamiltonian simulation. Finally, we conduct numerical simulations of the algorithm for solving linear systems of equations.

*Introduction.*—Quantum computing has wide applications in various linear algebra tasks. A prominent example is the quantum algorithm for solving linear systems of equations by Harrow, Hassidim, and Lloyd (HHL) in Ref. [1]. Given an  $N$  by  $N$  sparse matrix  $M$  and a state vector  $|v_0\rangle$ , the HHL quantum algorithm can prepare a state that is proportional to  $|v_M\rangle = M^{-1}|v_0\rangle$ , with a complexity polynomial in  $\log_2 N$  and condition number  $c$ , which is the ratio of the largest eigenvalue to the smallest eigenvalue of a given matrix. As classical algorithms generally have polynomial complexity in  $N$ , the HHL algorithm suggests exponential speed-ups of quantum computers. Recent developments of quantum algorithms for linear systems of equations can be found in Ref. [2–8]. Another common linear algebra task is matrix-vector multiplication by applying a sparse matrix  $M$  to a vector  $|v_0\rangle$  as  $|v_{M-1}\rangle = M|v_0\rangle$ . The quantum algorithms for linear equations can be similarly applied for matrix-vector multiplications. Furthermore, they can be applied for quantum optimisation and machine learning [9–11].

The conventional quantum algorithms generally require a long-depth circuit for a fault tolerant quantum computer. This is challenging for current technology. Recently, there has been great interest in quantum computing in the Noisy Intermediate Scaled Quantum (NISQ) regime, for finding energy spectra of a many-body Hamiltonian [12–23], simulating real and imaginary time dynamics of many-body systems [24–29], applications with machine learning [30–37], circuit learning [38–42], and others [43, 44]. These algorithms are generally hybrid in a sense that they only solve the core problem with a shallow quantum circuit and leave the higher level calculation to be performed with a classical computer. Furthermore, even without error correction, noise in the shallow circuit implementation can be suppressed via error mitigation [24, 45–52], indicating the feasibility of quantum

computing with NISQ hardware.

In this work, we propose variational algorithms for linear algebra problems, including linear systems of equations and matrix-vector multiplications, implemented with NISQ hardware. The main idea is to construct a many-body Hamiltonian so that its ground state corresponds to the solution of the linear algebra problem. Then we apply the recently proposed variational methods, such as variational quantum eigensolver (VQE) [12] or imaginary time evolution (ITE) [25, 26], to find the ground state and hence the solution. We also introduce Hamiltonian morphing with an adaptive ansatz to address the barren plateau problem [53]. Different from the conventional scenario where the ground state energy is generally unknown, the ground state energy of the linear algebra Hamiltonians is designed to be zero in our algorithms, and this further enables us to verify the correctness of the solution. Meanwhile, we show that the variational matrix-vector multiplication algorithm can be applied for Hamiltonian simulation as an alternative to the one proposed by Li and Benjamin [24]. Finally, we present numerical simulation results for solving linear systems of equations with random matrices that have sizes up to  $64^*64$ .

*Variational algorithms for linear algebra.*—We first introduce our variational algorithms for matrix-vector multiplication. Given a sparse  $N$  by  $N$  matrix  $M$  and an initial state vector  $|v_0\rangle$ , our task is to calculate the normalised state

$$|v_M\rangle = \frac{M|v_0\rangle}{\|M|v_0\rangle\|}, \quad (1)$$

with  $\|M|v_0\rangle\| = \langle v_0|M^\dagger M|v_0\rangle$ . Here, we consider the case that  $M$  can be a general (non-Hermitian) matrix. We find that  $|v_M\rangle$  is the ground state of the Hamiltonian

$$H_M = I - \frac{M|v_0\rangle\langle v_0|M^\dagger}{\|M|v_0\rangle\|^2}, \quad (2)$$

with energy 0. Using universal quantum computers, one may apply the conventional techniques [54, 55], such as adiabatic state preparation and phase estimation to find the ground state of  $H_M$ . With NISQ devices, we can instead consider the variational method with a parametrised state. The main idea is to first consider a state or ansatz,  $|\phi(\vec{\theta})\rangle = U(\vec{\theta})|0\rangle$ , with  $U(\vec{\theta}) = U_L(\theta_L) \dots U_2(\theta_2)U_1(\theta_1)$ ,  $\vec{\theta} = (\theta_1, \theta_2, \dots, \theta_L)$ . Suppose the ground state of  $H_M$  can be represented by the ansatz with certain parameters, the ground state finding problem is then converted to the minimisation,

$$\vec{\theta}_{\min} = \arg \min_{\vec{\theta}} \langle \phi(\vec{\theta}) | H_M | \phi(\vec{\theta}) \rangle, \quad (3)$$

with the solution given by  $|v_M\rangle = |\phi(\vec{\theta}_{\min})\rangle$ . The minimisation can be accomplished with various methods, such as gradient based classical optimisation VQE [12], global search algorithms [23], ITE [25, 26], etc. In the main text, we focus on the VQE method and leave the discussion of other method in Supplementary Materials. With VQE via gradient descent [12], we start with a guess of the solution,  $\vec{\theta}_0$  and update the parameters along the negative gradient of the energy  $E_M(\vec{\theta}) = \langle \phi(\vec{\theta}) | H_M | \phi(\vec{\theta}) \rangle$ ,

$$\vec{\theta}_{i+1} = \vec{\theta}_i - a \nabla E_M(\vec{\theta}_i), \quad \forall i = 0, 1, \dots, T \quad (4)$$

where  $a$  is the time step, and  $T$  is the total number of steps. As the energy  $E_M$  monotonically decreases with sufficiently small  $a$ , the solution via VQE always at least corresponds to a local minimum. Starting from several random initial positions, one may find the true solution, i.e., the global minimum. In conventional VQE, it is generally hard to verify whether the true ground state is achieved. As we will discuss shortly, we show that we can verify the correctness of the final state found.

Next, we consider the problem of solving linear equations. Given a sparse  $N$  by  $N$  matrix  $M$  and an initial state vector  $|v_0\rangle$ , we want to calculate

$$|v_{M^{-1}}\rangle = \frac{M^{-1}|v_0\rangle}{\|M^{-1}|v_0\rangle\|}, \quad (5)$$

where  $\|M^{-1}|v_0\rangle\| = \sqrt{\langle v_0 | M^{-1} M^{-1} | v_0 \rangle}$ . When the matrix  $M$  is not Hermitian, it can always be converted into an equivalent problem with a Hermitian matrix by doubling the number of qubits [1]. We therefore focus on the case where  $M$  is Hermitian and invertible. It is not hard to see that the solution  $|v_{M^{-1}}\rangle$  is the ground state of the Hamiltonian

$$H_{M^{-1}} = M^\dagger (I - |v_0\rangle \langle v_0|) M \quad (6)$$

with energy 0. Again, one can apply adiabatic algorithms to find the ground state with a universal quantum computer [8]. Here, we focus on the variational algorithm and consider the following optimisation problem

$$\vec{\theta}_{\min} = \arg \min_{\vec{\theta}} \langle \phi(\vec{\theta}) | H_{M^{-1}} | \phi(\vec{\theta}) \rangle, \quad (7)$$

with  $|v_{M^{-1}}\rangle = |\phi(\vec{\theta}_{\min})\rangle$ . With VQE, we start with a guess  $\vec{\theta}_0$  and update the parameters by

$$\vec{\theta}_{i+1} = \vec{\theta}_i - a \nabla E_{M^{-1}}(\vec{\theta}_i), \quad \forall i = 0, 1, \dots, T \quad (8)$$

with energy  $E_{M^{-1}}(\vec{\theta}) = \langle \phi(\vec{\theta}) | H_{M^{-1}} | \phi(\vec{\theta}) \rangle$ , time step  $a$ , and total number of steps  $T$ .

*Implementation with quantum circuits*—Now, we consider the implementation of our algorithms with quantum circuits. To realise the VQE optimisation, we need to obtain  $\nabla E_{M^{-1}}$  or  $\nabla E_M$ , which can be estimated either with the finite difference formulae or quantum gradient finding methods recently considered in Ref. [24, 56, 57]. For simplicity, we only focus on  $E = E_M$  in the main text and leave the discussion of  $E = E_{M^{-1}}$  in Supplementary Materials.

With the finite difference formulae, each component  $\partial E_M / \partial \theta_i$  of the gradient  $\nabla E_M = (\partial E_M / \partial \theta_i)$  around  $\vec{\theta}$  can be calculated as

$$\frac{\partial E_M}{\partial \theta_i} \approx \frac{E_M(\vec{\theta} + \delta \theta_i) - E_M(\vec{\theta} - \delta \theta_i)}{2\delta \theta_i}, \quad (9)$$

with  $\delta \theta_i \ll 1$ . Note that  $E_M(\vec{\theta}) = 1 - |\langle \phi(\vec{\theta}) | M | v_0 \rangle|^2$  with an arbitrary angle  $\vec{\theta}$ . Suppose  $M$  can be decomposed as  $M = \sum_j \lambda_j \sigma_j$ , we can then obtain  $E_M(\vec{\theta})$  as

$$E_M(\vec{\theta}) = 1 - \left| \sum_i \lambda_i \langle \phi(\vec{\theta}) | \sigma_i | v_0 \rangle \right|^2. \quad (10)$$

For each term, we denote  $\langle \phi(\vec{\theta}) | \sigma_i | v_0 \rangle = \langle 0 | U | 0 \rangle$  with  $U = U(\vec{\theta})^\dagger \sigma_i U_{v_0}$  and  $|v_0\rangle = U_{v_0} |0\rangle$ . The real and imaginary part of  $\langle \phi(\vec{\theta}) | \sigma_i | v_0 \rangle$  can be evaluated with the Hadamard test or swap test quantum circuits. Suppose  $M$  consists of a polynomial number (with respect to the number of qubits) of tensor products of local operators  $\sigma_j$ , we can then measure each term and efficiently calculate  $E_M(\vec{\theta})$ . Meanwhile, even if  $M = \sum_j \lambda_j \sigma_j$  has exponential terms with respect to the number of qubits, the algorithm is still efficient if we can efficiently sample the probability distribution  $|\lambda_i| / \sum_i |\lambda_i|$  with a polynomial dependence of  $\sum_i |\lambda_i|$  on the number of qubits. This includes cases where the coefficients have analytical expressions, which enables efficient sampling, or the matrix is an oracle-based sparse matrix.

With the quantum gradient finding method, we first express the gradient as

$$\frac{\partial E_M}{\partial \theta_i} = -2\Re \left( \frac{\partial \langle \phi(\vec{\theta}) |}{\partial \theta_i} M | v_0 \rangle \langle v_0 | M^\dagger | \phi(\vec{\theta}) \rangle \right). \quad (11)$$

The term  $\langle v_0 | M^\dagger | \phi(\vec{\theta}) \rangle$  can be efficiently measured with the aforementioned method. To measure  $\frac{\partial \langle \phi(\vec{\theta}) |}{\partial \theta_i} M | v_0 \rangle$ , we have to first decompose the derivative of the state as

$$\frac{\partial |\phi(\vec{\theta})\rangle}{\partial \theta_i} = \sum_s f_i^s |\phi_i^s(\vec{\theta})\rangle. \quad (12)$$

Here  $|\phi_i^s(\vec{\theta})\rangle = U_L(\theta_L)\dots\sigma_i^s U_i(\theta_i)\dots U_2(\theta_2)U_1(\theta_1)|0\rangle$ , and the derivative of the unitary is decomposed as  $\partial U_i(\theta_i)/\partial\theta_i = \sum_s f_i^s \sigma_i^s U_i(\theta_i)$  with tensor products of local operators  $\sigma_i^s$  and coefficients  $f_i^s$ . Then we have  $\frac{\partial\langle\phi(\vec{\theta})|M|v_0\rangle}{\partial\theta_i} = \sum_s f_i^{s*} \langle\phi_i^s(\vec{\theta})|M|v_0\rangle$  where each term can be efficiently measured with a quantum circuit.

*Solution verification.*—After finding the solution, it is also practically important to verify whether it is the correct one. This is in general impossible for conventional VQE as neither the ground state nor the ground state energy is known. However, we can verify the solution of the linear algebra problems as the exact solution should always have zero energy. We first consider the matrix-vector multiplication problem. With a solution  $|\phi(\vec{\theta}_{\min})\rangle$ , we can estimate  $|\langle\phi(\vec{\theta}_{\min})|v_M\rangle|^2$  via

$$|\langle\phi(\vec{\theta}_{\min})|v_M\rangle|^2 = 1 - E_M(\vec{\theta}_{\min}). \quad (13)$$

Therefore, we can also have the fidelity of  $|\phi(\vec{\theta}_{\min})\rangle$  to the exact solution  $|v\rangle$  from the energy  $E_M(\vec{\theta}_{\min})$  and the solution can be verified as correct whenever  $|\langle\phi(\vec{\theta}_{\min})|v\rangle|^2$  is close to 1.

Similarly, the solution of the linear equation can be verified by measuring the energy  $E_{M^{-1}}(\vec{\theta}_{\min})$  to be close to 0. Note that the fidelity  $|\langle\phi(\vec{\theta}_{\min})|v_{M^{-1}}\rangle|^2$  cannot be determined as we cannot directly measure  $|\langle\phi(\vec{\theta}_{\min})|M^{-1}|v_0\rangle|^2$  or  $\langle v_0|M^{-1}M^{-1}|v_0\rangle$ . Alternatively, we can verify the solution by checking whether  $|v_0\rangle \propto M|\phi(\vec{\theta}_{\min})\rangle$  is satisfied. Therefore, we can measure  $|\langle v_0|M|\phi(\vec{\theta}_{\min})\rangle|^2/\langle\phi(\vec{\theta}_{\min})|M^\dagger M|\phi(\vec{\theta}_{\min})\rangle$  and the solution is verified as correct when the value is close to 1. This can be an alternative cost function for VQE and we leave the discussion to future works.

*Optimisation via Hamiltonian morphing.*—The VQE method tries to find the global minimum of a large multi-parameter space. For each trial, one starts from a randomly initialised parameter set and obtains a local minimum after several optimisation steps. One can then verify whether the solution is correct by measuring the energy and restart from another random parameter set until the energy is close to 0. This may need to be repeated many times until a satisfactory solution can be found. There are several potential issues that can affect the practical performance. First, as the parameter space is large, it may require a large number of repetitions starting from different initial random parameters. This is a common issue in optimisation and machine learning, where a combination of different algorithms may help to speed up the search time. A more serious problem is that the gradient may vanish for randomly initialised parameters in some random quantum circuits of large systems [53]. In quantum computational chemistry, physically motivated ansatz and a good guess of initial parameters are considered to avoid vanishing gradient, see Refs. [58, 59] for recent reviews. However, this is not straightforward for the linear algebra tasks.

Here we propose a Hamiltonian morphing optimisation method to avoid these problems. Similar methods have been introduced in Refs. [60, 61] for variational quantum simulation. The morphing method is an analog to adiabatic state preparation, where one slowly varies the Hamiltonian from  $H_i$  to  $H_f$ , as to gradually evolve the corresponding ground state from  $|\psi_i\rangle$  to  $|\psi_f\rangle$ . For our morphing method, we consider the linear equation problem as an example and it works similarly for the matrix-vector multiplication problem. Denote a time-dependent Hamiltonian  $H_{M^{-1}}(t) = M(t)(I - |v_0\rangle\langle v_0|)M(t)$  with  $M(t)$  satisfying  $M(t=0) = I$  and  $M(t=T) = M$  respectively. Our algorithm starts from the ground state  $|v_0\rangle$  of  $H_{M^{-1}}(0)$  and reaches the ground state of the target Hamiltonian  $H_{M^{-1}}(T)$  as follows. Consider discretised time step  $\delta t$  and  $M(t) = (1 - t/T)I + t/T \cdot M$ .

1. At the  $n = 0$  step with time  $t = 0$ , we denote the parameters that represent  $|v_0\rangle$  as  $\vec{\theta}(0)$ , i.e.,  $|v_0\rangle = |\phi(\vec{\theta}(0))\rangle$ .
2. At the  $n^{\text{th}} \in [1, T/\delta t)$  step, we use parameters  $\vec{\theta}((n-1)\delta t)$  found in the last step for  $H_{M^{-1}}((n-1)\delta t)$  as the initial position to find parameters  $\vec{\theta}(n\delta t)$  that correspond to the ground state of  $H_{M^{-1}}(n\delta t)$ .

For any positive matrix  $M$ , when we use a sufficiently small  $\delta t$  and a powerful enough ansatz, our method is guaranteed to find the exact solution according to the adiabatic theorem [62]. For a general  $M$ , one can introduce an extra qubit so that the gap  $H_{M^{-1}}(t)$  is non-vanishing. We refer to Ref. [8] for details. In practice, the initially specified ansatz may not be powerful enough to represent the states at all time  $t$ . Fortunately, when the ansatz is insufficient at any time  $t$ , one can detect it by measuring a high averaged energy. Then one can either simply choose a more powerful ansatz or adaptively vary the ansatz by changing its structure and adding more gates [40]. Note that this is in general not possible for conventional many-body ground state problems with VQE, owing to the unknown ground state energy.

*Hamiltonian simulation.*—Our algorithms can be useful for tasks in quantum machine learning and optimisation. The matrix-vector multiplication algorithm can also be applied for variational Hamiltonian simulation. Starting from  $|\psi_0\rangle$ , the Hamiltonian simulation task is to prepare the state  $|\psi_t\rangle = e^{-iHt}|\psi_0\rangle$  at time  $t$  with sparse Hamiltonian  $H$ . For instance, when the Hamiltonian can be decomposed as a linear sum of polynomial terms  $H = \sum_j \lambda_j \sigma_j$ , we can make use of the Trotterization method to have

$$|\psi_t\rangle \approx \left( \prod_i e^{-i\lambda_j \sigma_j t/K} \right)^K |\psi_0\rangle + O(t^2/K), \quad (14)$$

with  $K$  Trotter steps. As the circuit depth increases with the evolution time, the circuit depth can be large for long evolution time. The variational quantum algorithm for simulating real-time dynamics with a constant circuit depth has been proposed by Li and Ben-

jamin [24]. Here, we present an alternative algorithm based on matrix-vector that can be more robust to the one in Ref. [24]. The key idea of Ref. [24] is to prepare the state at any time  $t$  via a parametrised state  $|\phi(\vec{\theta}(t))\rangle$  and update the parameters from  $\vec{\theta}(t)$  to  $\vec{\theta}(t + \delta t)$  that effectively realise  $e^{-iH\delta t}|\phi(\vec{\theta}(t))\rangle$  via a deterministic process  $\vec{\theta}(t + \delta t) = \vec{\theta}(t) + \dot{\vec{\theta}}(t)\delta t$  with  $\dot{\vec{\theta}}(t) = A^{-1}C$ , where  $A_{i,j}(t) = -\text{Im}\left(\frac{\partial\langle\phi(\vec{\theta})|}{\partial\theta_i}\frac{\partial|\phi(\vec{\theta})\rangle}{\partial\theta_j}\right)$  and  $C_i(t) = \text{Re}\left(\frac{\partial\langle\phi(\vec{\theta})|}{\partial\theta_i}H|\phi(\vec{\theta})\rangle\right)$ . Each term of  $A$  and  $C$  can be efficiently measured via a quantum circuit.

Instead of deterministically obtaining  $\vec{\theta}(t + \delta t)$  via  $\dot{\vec{\theta}}(t)$ , we make use of the algorithm introduced in this paper. That is, to realise  $e^{-iH\delta t}|\phi(\vec{\theta}(t))\rangle$ , we can consider  $M = e^{-iH\delta t} \approx 1 - iH\delta t$  and update the parameters as  $|\phi(\vec{\theta}(t + \delta t))\rangle = M|\phi(\vec{\theta}(t))\rangle$ . Therefore, for each time step, we can update the parameters according to the matrix-vector algorithm.

*Numerical simulation.*—We numerically test the variational algorithm for solving linear systems of equations. The simulation is based on the Quantum Exact Simulation Toolkit (QuEST) package [63], which is a high performance classical simulator of general quantum circuits. In our simulation, we consider  $2^n$  by  $2^n$  positive complex Hermitian matrices  $M$  with  $n$  qubits. Note that even though the matrix size is assumed to be an exponential of 2, an  $m$  by  $m$  matrix with  $2^{n-1} < m \leq 2^n$  can be also handled with an  $n$ -qubit circuit. The matrix is randomly generated with a given condition number  $c$  and the input state is also randomly generated. As we use no prior information of the matrix, we consider the ansatz as shown in Fig. 1, where each green blocks  $V_i$  has a fixed structure. We also vary the number of blocks, called the circuit depth  $m$ , to endow the ansatz with different powers. In a more practical scenario, we can assume that we have a sparse decomposition of the matrix and the input state is simple to prepare or it is obtained from a previous calculation. We can also try different ansätze such as the Hamiltonian ansatz, defined based on the Pauli decomposition of the matrix. As this work only aims to verify the basic function of the algorithm, we leave the simulation of the practical cases to a future work.

We also implement the optimisation based on Hamiltonian morphing with an adaptive ansatz. We divide the total time  $T$  into 10 intervals with an equal duration, where  $T$  ranges from 20 to 100 depending on the matrix size. At  $t = 0$ , we set  $H_{M-1} = I - |v_0\rangle\langle v_0|$  with the ground state being the input state  $|v_0\rangle$  and start with all single-qubit gates parameterised with a small random rotation angle. In the  $i^{\text{th}}$  variational cycle, the gradient descent method is used to search for the ground state energy of a time-dependent Hamiltonian  $H_{M-1}(t) = M(t)(I - |v_0\rangle\langle v_0|)M(t)$  with  $M(t) = (1 - i/10)I + i/10 \cdot M$ , and a step size  $\delta t = 0.1$ . We choose initial parameters to be the ones obtained from

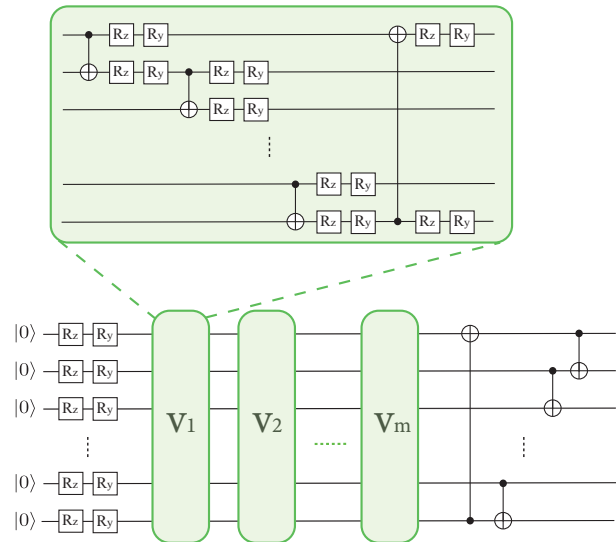


FIG. 1. The circuit ansatz. In total  $n$  qubits are required to solve a problem with a  $2^n * 2^n$  matrix. Here,  $R_y$  and  $R_z$  represent single qubit rotations around the  $Y$  and  $Z$  axes, respectively. The rotation angle (parameter) for each single-qubit gate is initialised from a small random value, which is updated in each of the variational cycle. At the beginning two single-qubit gates are applied to each of the data qubit, followed with sets of CNOT gates, as depicted as the green block  $V$ . Within each set, a CNOT gate is followed with two single-qubit gates. The number of sets represents the depth of the circuit, which is gradually increased until a desired target state is found. In the end, a set of CNOT gates is applied, which is in the reversed order as in  $V$ . The aim for this set is to ensure that the eigenstate can be found at  $t = 0$ , when the Hamiltonian morphing technique is applied.

the previous cycle. A small circuit depth  $m$  is tried at the beginning and is increased gradually until the fidelity of the qubit state to the target state is higher than 99%, which is regarded as a success.

We study the complexity of our algorithm with respect to the matrix size and the condition number of the matrix. We first fix the matrix size to be  $2^6 * 2^6$  with 6 qubits and consider random matrices with different condition numbers. For different condition numbers from 10 to 100, we test our algorithm with different circuit depth. For each case, we run 4940 random trials to calculate the averaged success probability with results shown in Fig. 2. Not surprisingly, we found that a larger circuit depth ansatz generally leads to a higher success probability. We also obtain the minimum depth that is required to guarantee the success of finding  $|v_{M-1}\rangle$ , plotted as an insert. Overall, we find that the minimal required depth varies linearly with the condition number.

Next, we vary the size  $2^n * 2^n$  of the matrix  $M$ , by changing the number of data qubits  $n$  in the circuit ansatz. For an  $n$ -qubit system, the condition number is

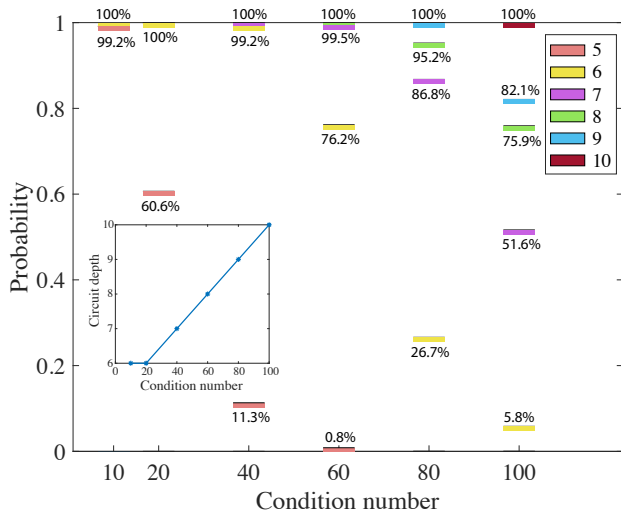


FIG. 2. The probability to find the target state with increasing condition number and circuit depths. This experiment is based on a 6-qubit circuit, thus the matrix size is fixed to be  $64 \times 64$ . For a given condition number, the success (having a solution with a fidelity higher than 99%) probability is shown for the circuit with increasing depths, until it reaches 100% (i.e., all the 4940 runs). The minimum depth required to find the target state with 100% success probability is plotted in the inserted graph.

adopted as  $c = 10n$ . As shown in Fig. 3, the circuit depth leading to a non-zero success probability also increases with respect to the number of qubits. The inserted plot shows the minimum circuit depth for achieving a 100% success probability. Overall, we find a super-linear increase of the circuit depth with respect to the number of qubits.

This is not surprising as we consider random matrices with random input states. Even though we consider fixed condition numbers, it only determines properties of eigenvalues of the matrix. For any matrix  $M$ , all other matrices  $UMU^\dagger$  with unitary  $U$  have the same eigenvalues and hence the same condition number. As the unitary  $U$  is an arbitrary unitary, it can lead to a general solution state, which may not be able to be prepared with shallow circuits. This explains the super-linear dependence of the circuit depth with respect to the number of qubits. One possible solution to this problem is to consider sparse matrices as in Ref. [1]. Meanwhile, a better ansatz whose design is informed by the matrix can be designed. For example, we note that the chosen ansatz is not optimal for the problem, and a much more compact one can be obtained from circuit compiling [40] as shown in the Supplementary Materials. As our algorithm has the capability of verifying the solution, it also enables us to dynamically varying the ansatz until the solution is found. In our simulation, we dynamically increase the circuit depth and we expect more profound circuit mor-

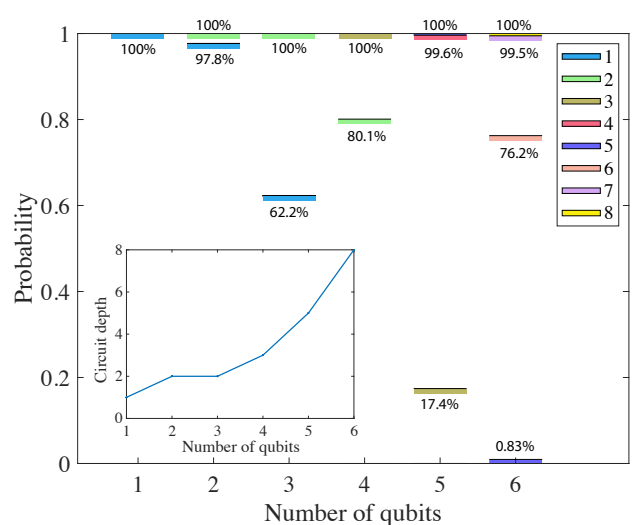


FIG. 3. The probability to find the target state with increasing number of qubits and circuit depths. For a given number of qubits, circuit depth is increased gradually until the probability reaches 1. The inserted graph shows the minimum depth found in the simulation when the target state is found with 100% probability.

phing techniques can be designed and exploited.

*Discussion.*—In this work we present variational algorithms for solving linear algebra problems including linear system of equations and matrix-vector multiplications with NISQ devices. We design a Hamiltonian with the ground state as the solution of the target problem, and solve it with the recently-proposed variational algorithms. As the ground state has zero energy, it also enables us to verify the solution and adjust the ansatz. We also introduce the Hamiltonian morphing technique to avoid local minima and to accelerate the search progress, and numerically verify our algorithm for solving the linear systems of equations. Owing to computation limitations, we consider randomly chosen matrices with a small range of matrix size. Within this range and with the non-optimal ansatz, the result suggests that the circuit depth based on our algorithm scales linearly with the condition number and super-linearly with the number of qubits. We expect further improvements of the performance of the algorithm for sparse matrices together with more sophisticated ansätze. We also expect that our results may shed light on quantum machine learning and quantum optimisations in the NISQ era.

## ACKNOWLEDGEMENTS.

This work is supported by the EPSRC National Quantum Technology Hub in Networked Quantum Information Technology (EP/M013243/1). SE is supported by

Japan Student Services Organization (JASSO) Student Exchange Support Program (Graduate Scholarship for Degree Seeking Students). YL is supported by NSAF (Grant No. U1730449).

---

\* xiao.yuan.ph@gmail.com

- [1] A. W. Harrow, A. Hassidim, and S. Lloyd, *Phys. Rev. Lett.* **103**, 150502 (2009).
- [2] A. Childs, R. Kothari, and R. Somma, *SIAM Journal on Computing* **46**, 1920 (2017), <https://doi.org/10.1137/16M1087072>.
- [3] A. Ambainis, in *STACS'12 (29th Symposium on Theoretical Aspects of Computer Science)*, Vol. 14 (LIPIcs, 2012) pp. 636–647.
- [4] B. D. Clader, B. C. Jacobs, and C. R. Sprouse, *Phys. Rev. Lett.* **110**, 250504 (2013).
- [5] L. Wossnig, Z. Zhao, and A. Prakash, *Phys. Rev. Lett.* **120**, 050502 (2018).
- [6] S. Chakraborty, A. Gilyén, and S. Jeffery, arXiv preprint arXiv:1804.01973 (2018).
- [7] A. Gilyén, Y. Su, G. H. Low, and N. Wiebe, arXiv preprint arXiv:1806.01838 (2018).
- [8] Y. b. u. Subaşı, R. D. Somma, and D. Orsucci, *Phys. Rev. Lett.* **122**, 060504 (2019).
- [9] P. Reberntrost, M. Mohseni, and S. Lloyd, *Phys. Rev. Lett.* **113**, 130503 (2014).
- [10] S. Lloyd, M. Mohseni, and P. Reberntrost, *Nature Physics* **10**, 631 (2014).
- [11] J. Biamonte, P. Wittek, N. Pancotti, P. Reberntrost, N. Wiebe, and S. Lloyd, *Nature* **549**, 195 (2017).
- [12] A. Peruzzo, J. McClean, P. Shadbolt, M.-H. Yung, X.-Q. Zhou, P. J. Love, A. Aspuru-Guzik, and J. L. O'Brien, *Nature communications* **5** (2014).
- [13] Y. Wang, F. Dolde, J. Biamonte, R. Babbush, V. Bergholm, S. Yang, I. Jakobi, P. Neumann, A. Aspuru-Guzik, J. D. Whitfield, *et al.*, *ACS nano* **9**, 7769 (2015).
- [14] P. J. J. O'Malley, R. Babbush, I. D. Kivlichan, J. Romero, J. R. McClean, R. Barends, J. Kelly, P. Roushan, A. Tranter, N. Ding, B. Campbell, Y. Chen, Z. Chen, B. Chiaro, A. Dunsworth, A. G. Fowler, E. Jeffrey, E. Lucero, A. Megrant, J. Y. Mutus, M. Neeley, C. Neill, C. Quintana, D. Sank, A. Vainsencher, J. Wenner, T. C. White, P. V. Coveney, P. J. Love, H. Neven, A. Aspuru-Guzik, and J. M. Martinis, *Phys. Rev. X* **6**, 031007 (2016).
- [15] Y. Shen, X. Zhang, S. Zhang, J.-N. Zhang, M.-H. Yung, and K. Kim, *Phys. Rev. A* **95**, 020501 (2017).
- [16] J. R. McClean, J. Romero, R. Babbush, and A. Aspuru-Guzik, *New Journal of Physics* **18**, 023023 (2016).
- [17] S. Paesani, A. A. Gentile, R. Santagati, J. Wang, N. Wiebe, D. P. Tew, J. L. O'Brien, and M. G. Thompson, *Phys. Rev. Lett.* **118**, 100503 (2017).
- [18] J. I. Colless, V. V. Ramasesh, D. Dahlen, M. S. Blok, M. E. Kimchi-Schwartz, J. R. McClean, J. Carter, W. A. de Jong, and I. Siddiqi, *Phys. Rev. X* **8**, 011021 (2018).
- [19] R. Santagati, J. Wang, A. A. Gentile, S. Paesani, N. Wiebe, J. R. McClean, S. Morley-Short, P. J. Shadbolt, D. Bonneau, J. W. Silverstone, D. P. Tew, X. Zhou, J. L. O'Brien, and M. G. Thompson, *Science Advances* **4** (2018), 10.1126/sciadv.aap9646.
- [20] A. Kandala, A. Mezzacapo, K. Temme, M. Takita, M. Brink, J. M. Chow, and J. M. Gambetta, *Nature* **549**, 242 (2017).
- [21] A. Kandala, K. Temme, A. D. Corcoles, A. Mezzacapo, J. M. Chow, and J. M. Gambetta, arXiv:1805.04492 (2018).
- [22] C. Hempel, C. Maier, J. Romero, J. McClean, T. Monz, H. Shen, P. Jurcevic, B. P. Lanyon, P. Love, R. Babbush, A. Aspuru-Guzik, R. Blatt, and C. F. Roos, *Phys. Rev. X* **8**, 031022 (2018).
- [23] C. Kokail, C. Maier, R. van Bijnen, T. Brydges, M. K. Joshi, P. Jurcevic, C. A. Muschik, P. Silvi, R. Blatt, C. F. Roos, and P. Zoller, *Nature (London)* **569**, 355 (2019), arXiv:1810.03421 [quant-ph].
- [24] Y. Li and S. C. Benjamin, *Phys. Rev. X* **7**, 021050 (2017).
- [25] S. McArdle, T. Jones, S. Endo, Y. Li, S. C. Benjamin, and X. Yuan, *npj Quantum Information* **5**, 75 (2019).
- [26] X. Yuan, S. Endo, Q. Zhao, S. Benjamin, and Y. Li, arXiv e-prints, arXiv:1812.08767 (2018), arXiv:1812.08767 [quant-ph].
- [27] S. Endo, Y. Li, S. Benjamin, and X. Yuan, arXiv preprint arXiv:1812.08778 (2018).
- [28] K. Heya, K. M. Nakanishi, K. Mitarai, and K. Fujii, arXiv e-prints, arXiv:1904.08566 (2019), arXiv:1904.08566 [quant-ph].
- [29] M.-C. Chen, M. Gong, X.-S. Xu, X. Yuan, J.-W. Wang, C. Wang, C. Ying, J. Lin, Y. Xu, Y. Wu, *et al.*, arXiv preprint arXiv:1905.03150 (2019).
- [30] J. Romero, J. P. Olson, and A. Aspuru-Guzik, *Quantum Science and Technology* **2**, 045001 (2017).
- [31] E. Farhi and H. Neven, arXiv preprint arXiv:1802.06002 (2018).
- [32] A. Perdomo-Ortiz, M. Benedetti, J. Realpe-Gómez, and R. Biswas, *Quantum Science and Technology* **3**, 030502 (2018).
- [33] M. Benedetti, D. Garcia-Pintos, O. Perdomo, V. Leyton-Ortega, Y. Nam, and A. Perdomo-Ortiz, arXiv preprint arXiv:1801.07686 (2018).
- [34] V. Havlíček, A. D. Corcoles, K. Temme, A. W. Harrow, A. Kandala, J. M. Chow, and J. M. Gambetta, *Nature* **567**, 209 (2019).
- [35] L. Lamata, U. Alvarez-Rodriguez, J. D. Martín-Guerrero, M. Sanz, and E. Solano, *Quantum Science and Technology* **4**, 014007 (2018).
- [36] A. Khoshaman, W. Vinci, B. Denis, E. Andriyash, and M. H. Amin, *Quantum Science and Technology* **4**, 014001 (2018).
- [37] S. Lloyd and C. Weedbrook, *Physical review letters* **121**, 040502 (2018).
- [38] K. Mitarai, M. Negoro, M. Kitagawa, and K. Fujii, *Physical Review A* **98**, 032309 (2018).
- [39] L. Cincio, Y. Subaşı, A. T. Sornborger, and P. J. Coles, *New Journal of Physics* **20**, 113022 (2018).
- [40] T. Jones and S. C. Benjamin, arXiv preprint arXiv:1811.03147 (2018).
- [41] J. Biamonte, arXiv e-prints, arXiv:1903.04500 (2019), arXiv:1903.04500 [quant-ph].
- [42] K. Sharma, S. Khatri, M. Cerezo, and P. J. Coles, arXiv preprint arXiv:1908.04416 (2019).
- [43] M. Lubasch, J. Joo, P. Moinier, M. Kiffner, and D. Jaksch, arXiv e-prints, arXiv:1907.09032 (2019), arXiv:1907.09032 [quant-ph].

- [44] Y. Lee, J. Joo, and S. Lee, *Scientific reports* **9**, 4778 (2019).
- [45] J. R. McClean, M. E. Kimchi-Schwartz, J. Carter, and W. A. de Jong, *Phys. Rev. A* **95** (2017).
- [46] K. Temme, S. Bravyi, and J. M. Gambetta, *Phys. Rev. Lett.* **119**, 180509 (2017).
- [47] S. Endo, S. C. Benjamin, and Y. Li, *Physical Review X* **8**, 031027 (2018).
- [48] J. Colless, V. Ramasesh, D. Dahlen, M. Blok, M. Kimchi-Schwartz, J. McClean, J. Carter, W. de Jong, and I. Siddiqi, *Phys. Rev. X* **8** (2018).
- [49] M. Otten and S. Gray, arXiv preprint arXiv:1806.07860 (2018).
- [50] S. Endo, Q. Zhao, Y. Li, S. Benjamin, and X. Yuan, *Phys. Rev. A* **99**, 012334 (2019).
- [51] S. McArdle, X. Yuan, and S. Benjamin, arXiv preprint arXiv:1807.02467 (2018).
- [52] X. Bonet-Monroig, R. Sagastizabal, M. Singh, and T. O'Brien, arXiv preprint arXiv:1807.10050 (2018).
- [53] J. R. McClean, S. Boixo, V. N. Smelyanskiy, R. Babbush, and H. Neven, *Nature communications* **9**, 4812 (2018).
- [54] D. S. Abrams and S. Lloyd, *Phys. Rev. Lett.* **79**, 2586 (1997).
- [55] A. Aspuru-Guzik, A. D. Dutoi, P. J. Love, and M. Head-Gordon, *Science* **309**, 1704 (2005).
- [56] P.-L. Dallaire-Demers, J. Romero, L. Veis, S. Sim, and A. Aspuru-Guzik, arXiv preprint arXiv:1801.01053 (2018).
- [57] J. Romero, R. Babbush, J. R. McClean, C. Hempel, P. J. Love, and A. Aspuru-Guzik, *Quantum Science and Technology* **4**, 014008 (2018).
- [58] S. McArdle, S. Endo, A. Aspuru-Guzik, S. Benjamin, and X. Yuan, arXiv preprint arXiv:1808.10402 (2018).
- [59] Y. Cao, J. Romero, J. P. Olson, M. Degroote, P. D. Johnson, M. Kieferová, I. D. Kivlichan, T. Menke, B. Peropadre, N. P. Sawaya, *et al.*, arXiv preprint arXiv:1812.09976 (2018).
- [60] D. Wecker, M. B. Hastings, and M. Troyer, *Phys. Rev. A* **92**, 042303 (2015).
- [61] A. Garcia-Saez and J. I. Latorre, arXiv:1806.02287 (2018).
- [62] T. Albash and D. A. Lidar, *Rev. Mod. Phys.* **90**, 015002 (2018).
- [63] T. Jones, A. Brown, I. Bush, and S. C. Benjamin, *Scientific Reports* **9**, 10736 (2019).

### The lowest eigenstate of $H_{M^{-1}}$

Here, we show the lowest eigenstate of  $H_{M^{-1}}$  is  $M^{-1}|v_0\rangle$ . For an arbitrary vector  $|\varphi\rangle$ ,

$$\langle\varphi|H_{M^{-1}}|\varphi\rangle = \langle\varphi|M(I - |v_0\rangle\langle v_0|)M|\varphi\rangle \quad (15)$$

$$= \sum_i |\langle\varphi|M|\varphi_i\rangle|^2 \geq 0, \quad (16)$$

where we denoted  $I - |v_0\rangle\langle v_0| = \sum_i |\varphi_i\rangle\langle\varphi_i|$ ,  $\langle\varphi_i|\varphi_j\rangle = \delta_{i,j}$ . Therefore  $H_{M^{-1}}$  is a positive semidefinite matrix. On the other hand,  $H_{M^{-1}}M^{-1}|v_0\rangle = 0$ , thus  $M^{-1}$  is the lowest eigenvector of  $H_{M^{-1}}$ .

### Optimisation methods searching for $\vec{\theta}_{min}$

Search for the optimal set of parameters based on the cost function can be generalised as an optimisation problem, which can be handled with many methods. We describe the approach of imaginary time evolution approach [26] here. Based on the McLachlans variational principle, the minimisation starts with a initial guess of parameters  $\vec{\theta}_0$ , which is to be updated in each cycle with its derivative given by:

$$\sum_j M_{i,j}\dot{\theta}_j = -V_i, \quad (17)$$

where

$$M_{i,j} = \Re\left(\frac{\partial\langle\phi(\vec{\theta})|\partial\phi(\vec{\theta})}{\partial\theta_i}\frac{\partial\phi(\vec{\theta})}{\partial\theta_j}\right), \quad V_i = \Re\left(\frac{\partial\langle\phi(\vec{\theta})|H|\phi(\vec{\theta})\rangle}{\partial\theta_i}\right). \quad (18)$$

The Hamiltonian  $H$  for the two cases described in the main text would be  $H_M$  and  $H_{M^{-1}}$  respectively. By updating  $\vec{\theta}$  via:

$$\vec{\theta}_{i+1} = \vec{\theta}_i + \Delta T\dot{\vec{\theta}}_i \quad (19)$$

with a sufficiently small time step  $\Delta T$ , the corresponding energy  $E_M$  or  $E_{M^{-1}}$  would decrease along the optimisation trajectory.

### Circuit implementation of $\nabla E_{M^{-1}}$

Here we show that the circuits to implement  $\nabla E_{M^{-1}}$  can be found similarly as we do for  $\nabla E_M$ . We have

$$H_{M^{-1}} = M^\dagger(I - |v_0\rangle\langle v_0|)M, \quad (20)$$

thus

$$\begin{aligned} \frac{\partial E_{M^{-1}}}{\partial\theta_i} &= \frac{\partial}{\partial\theta_i}(\langle\phi(\vec{\theta})|H_{M^{-1}}|\phi(\vec{\theta})\rangle) = 2\Re\left(\frac{\partial\langle\phi(\vec{\theta})|H|\phi(\vec{\theta})\rangle}{\partial\theta_i}\right) \\ &= 2\Re\left(\frac{\partial\langle\phi(\vec{\theta})|M^\dagger M|\phi(\vec{\theta})\rangle}{\partial\theta_i}\right) - 2\Re\left(\frac{\partial\langle\phi(\vec{\theta})|M^\dagger|v_0\rangle\langle v_0|M|\phi(\vec{\theta})\rangle}{\partial\theta_i}\right). \end{aligned} \quad (21)$$

Suppose  $M$  can be decomposed into combinations of Pauli terms  $M = \sum_j \alpha_j \sigma_j$ ,  $M^\dagger M$  can then be expressed as  $M^\dagger M = \sum_j \beta_j \sigma_j$ , where the coefficients  $\alpha$  and  $\beta$  for each term are different. We decompose the derivative of the state as

$$\frac{\partial|\phi(\vec{\theta})\rangle}{\partial\theta_i} = \sum_s f_i^s |\phi_i^s(\vec{\theta})\rangle, \quad (22)$$

the same way as described in the main text. Then the first term in Equation 21 is expressed as

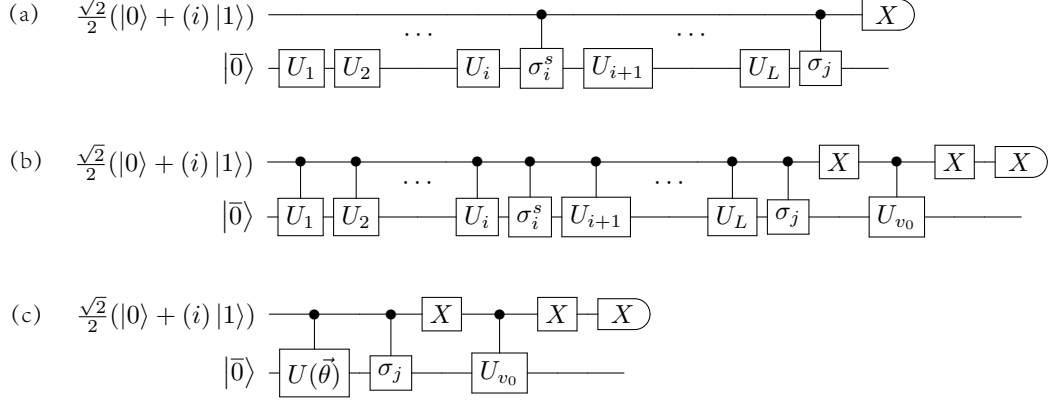


FIG. 4. The circuits to implement  $\nabla E_{M-1}$ . The first qubit is the ancilla, and the second refers to the data qubit register. The real part can be obtained from measuring  $\langle X \rangle$  when the ancilla initialised at  $\frac{\sqrt{2}}{2}(|0\rangle + |1\rangle)$ , while the imaginary part is evaluated if the ancilla is initialised at  $\frac{\sqrt{2}}{2}(|0\rangle + i|1\rangle)$ .

$$\begin{aligned} \frac{\partial \langle \phi(\vec{\theta}) |}{\partial \theta_i} M^\dagger M |\phi(\vec{\theta})\rangle &= \sum_s f_i^{s*} \langle \phi_i^s(\vec{\theta}) | M^\dagger M |\phi(\vec{\theta})\rangle \\ &= \sum_j \sum_s c_i^{s,j} \langle 0 | U_1^\dagger(\theta_1) U_2^\dagger(\theta_2) \dots U_i^\dagger(\theta_i) \sigma_i^s \dots U_L^\dagger(\theta_L) \sigma_j U_L(\theta_L) \dots U_2(\theta_2) U_1(\theta_1) | 0 \rangle. \end{aligned} \quad (23)$$

The real and imaginary value of each term  $\langle 0 | U_1^\dagger(\theta_1) U_2^\dagger(\theta_2) \dots U_i^\dagger(\theta_i) \sigma_i^s \dots U_L^\dagger(\theta_L) \sigma_j U_L(\theta_L) \dots U_2(\theta_2) U_1(\theta_1) | 0 \rangle$  can be evaluated with the circuit shown in Figure 4(a), by initialising the ancilla qubit to be at  $\frac{\sqrt{2}}{2}(|0\rangle + |1\rangle)$  and  $\frac{\sqrt{2}}{2}(|0\rangle + i|1\rangle)$  respectively.

The second term can be separated as two parts,  $\frac{\partial \langle \phi(\vec{\theta}) |}{\partial \theta_i} M^\dagger |v_0\rangle$  and  $\langle v_0 | M |\phi(\vec{\theta})\rangle$ . The first part can be expressed as

$$\begin{aligned} \frac{\partial \langle \phi(\vec{\theta}) |}{\partial \theta_i} M^\dagger |v_0\rangle &= \sum_s f_i^{s*} \langle \phi_i^s(\vec{\theta}) | M^\dagger U_{v_0} |0\rangle \\ &= \sum_j \sum_s d_i^{s,j} \langle 0 | U_1^\dagger(\theta_1) U_2^\dagger(\theta_2) \dots U_i^\dagger(\theta_i) \sigma_i^s \dots U_L^\dagger(\theta_L) \sigma_j U_{v_0} |0\rangle, \end{aligned} \quad (24)$$

where each term can be evaluated with the circuit shown in Figure 4(b). The second part is written as

$$\langle v_0 | M |\phi(\vec{\theta})\rangle = \langle 0 | U_{v_0}^\dagger M U(\vec{\theta}) |0\rangle = \sum_j k_j \langle 0 | U_{v_0}^\dagger \sigma_j U(\vec{\theta}) |0\rangle \quad (25)$$

where each term can be evaluated with the circuit shown in Figure 4(c).

### Example with a more compact circuit

In this paper we apply the hardware-efficient ansatz for practical soundness, however, this is not the optimal ansatz for most cases. Here we take one case as an example, where the solution is found difficult to reach in our numerical simulations.

The matrix in this case is a complex matrix with size of  $64 \times 64$ , and condition number  $c = 60$ .  $|v_0\rangle$  is a complex vector, and the target state is  $|v_{M-1}\rangle = \frac{M^{-1}|v_0\rangle}{\|M^{-1}|v_0\rangle\|}$ . It is found in the numerical simulation that the target state can not be represented by a circuit with depth 7 but can by a circuit with depth 8. On the other hand, applying quantum compiling, it is found that the target state can be realised with a circuit that requires only half the number of parameters. Figure 5 is one example of the circuits found to prepare a state with fidelity higher than 99.9% compared

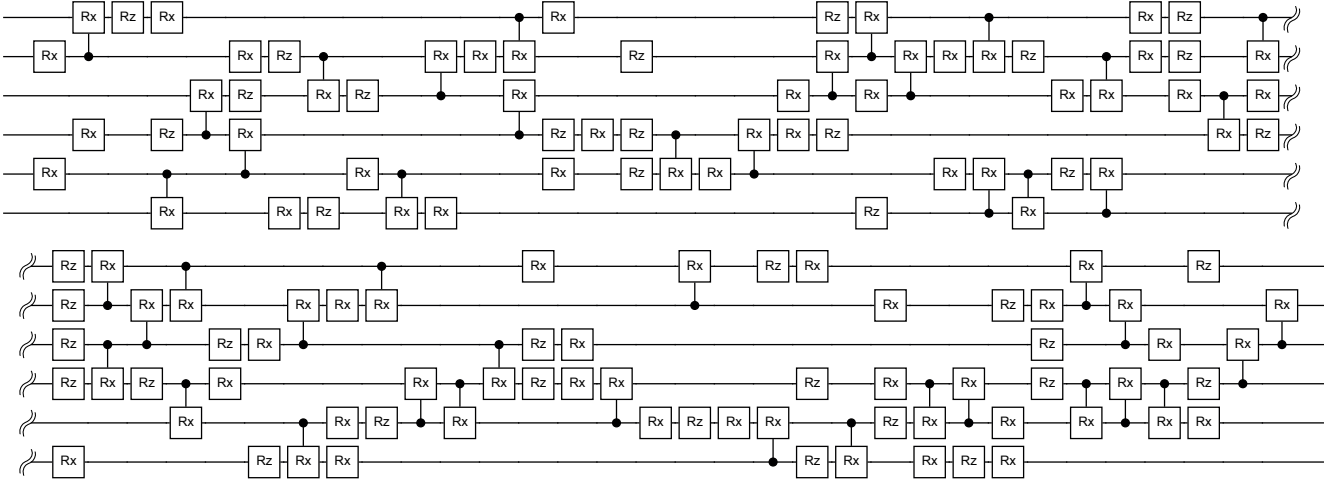


FIG. 5. A more compact circuit found with quantum compilation to realise the target state. Each single- and multi-qubit gate is controlled with one parameter. In total 126 parameters are included in the circuit, which realises the state with a fidelity higher than 99.9%.

with the target state. A limited topology with only nearest-neighbor interactions is considered here as it is more hardware efficient. The detailed description and the parameters can be found at <https://questlink.qtechtheory.org/>.